THE JOURNAL OF PHYSICAL CHEMISTRY LETTERS
A JOURNAL OF THE AMERICAN CHEMICAL SOCIETY

pubs.acs.org/JPCL

Letter

Sterically Suppressed Phase Segregation in 3D Hollow Mixed-Halide Wide Band Gap Perovskites

Luke Grater, Mingcong Wang, Sam Teale, Suhas Mahesh, Aidan Maxwell, Yanjiang Liu, So Min Park, Bin Chen, Frédéric Laquai, Mercouri G. Kanatzidis, and Edward H. Sargent*

Cite This: J. Phys. Chem. Lett. 2023, 14, 6157−6162

Read Online

ACCESS | Metrics & More | Article Recommendations | Supporting Information

ABSTRACT: Band gap tuning in mixed-halide perovskites enables efficient multijunction solar cells and LEDs. However, these wide band gap perovskites, which contain a mixture of iodide and bromide ions, are known to phase segregate under illumination, introducing voltage losses that limit stability. Previous studies have employed inorganic perovskites, halide alloys, and grain/interface passivation to minimize halide segregation, yet photostability can be further advanced. By focusing on the role of halide vacancies in anion migration, one expects to be able to erect local barriers to ion migration. To achieve this, we employ a 3D "hollow" perovskite structure, wherein a molecule that is otherwise too large for the perovskite lattice is incorporated. The amount of hollowing agent, ethane-1,2-diammonium dihydroiodide (EDA), varies the density of the hollow sites. Photoluminescence measurements reveal that 1% EDA in the perovskite bulk can stabilize a 40% bromine mixed-halide perovskite at 1 sun illumination intensity. These, along with capacitance−frequency measurements, suggest that hollow sites limit the mobility of the halide vacancies.

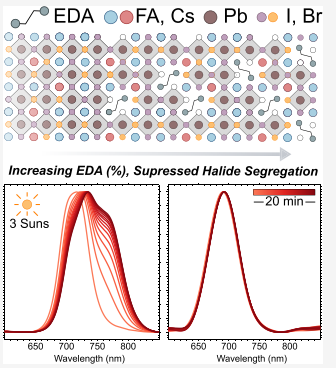

Metal halide perovskites have attracted significant attention due to their band gap tunability through alloying, achieved by varying the ratio of I to Br in $AB(I_xBr_{1-x})_3$,[1] where the A-site cation is typically an alloy of MA, FA, or Cs and the B-site cation is Pb or Sn.

When the Br content exceeds 20%, mixed-halide perovskites segregate upon exposure to light, forming I-rich domains with a band gap lower than in their parent mixed phase.[2] Higher than 20% Br content is needed for efficient perovskite−perovskite tandem solar cells, but the performance remains hindered by halide segregation. Photogenerated carriers tend to accumulate in these low-energy regions, limiting the open-circuit voltage and thus the efficiency of multijunction cells.[3−5]

Prior experimental studies correlate phase segregation with defect densities,[6] motivating many prior contributions to focus on minimizing these through A- and X-site compositional tuning and grain passivation.[7−10] Adjusting the A-site and X-site compositions, such as with Cs and Cl, has increased the resistance to segregation,[7,8] as has the passivation of electronic trap states, especially those at the absorber/transport-layer interface.[11]

Opportunities nevertheless remain to increase the range and stability of compositions further, including in >40% Br materials with the goal of withstanding accelerated aging conditions such as illumination above 3 suns.

Our concept here was to introduce local steric barriers against ion migration, reducing the mobility of vacancies believed to facilitate detrimental ion migration. We explore implementing this idea in hollow perovskites, a class of materials previously used to tune the optoelectronic properties of 3D perovskites.[12,13] A large divalent cation, such as ethylenediammonium (EDA), is included in the perovskite ABX_3 structure, expelling other atoms from the lattice: B- and X-site vacancies. In contrast to the case of 2D perovskites, the lattice retains its 3D structure, which is promising for the retention of reasonable charge transport.[12] Hollow sites in the lattice have previously been shown to increase the chemical and kinetic stability,[12] again suggesting promise in mitigating ion migration associated with phase segregation.

Prior studies report hollow perovskite structures in single crystals and films of monohalide, pure Pb, and mixed Pb-Sn perovskites.[12−16] Here we use EDA to incorporate a 3D hollow structure into pure Pb mixed-halide thin films. We fabricated thin films of mixed-halide hollow perovskite by incorporating the hollowing agent, EDA, into a $Cs_{0.17}FA_{0.83}Pb(I_{0.6}Br_{0.4})_3$ mixed-halide wide band gap precursor solution at varying molar percentages depending on the experiment (ranging from 0.5 to 10%). The precursor solution was then spin-coated onto substrates and annealed (details in Methods). We spin-coated a poly(methyl methacrylate) (PMMA) layer on top of the annealed films.[17]

Received: April 27, 2023
Accepted: June 20, 2023

https://doi.org/10.1021/acs.jpclett.3c01156
J. Phys. Chem. Lett. 2023, 14, 6157−6162

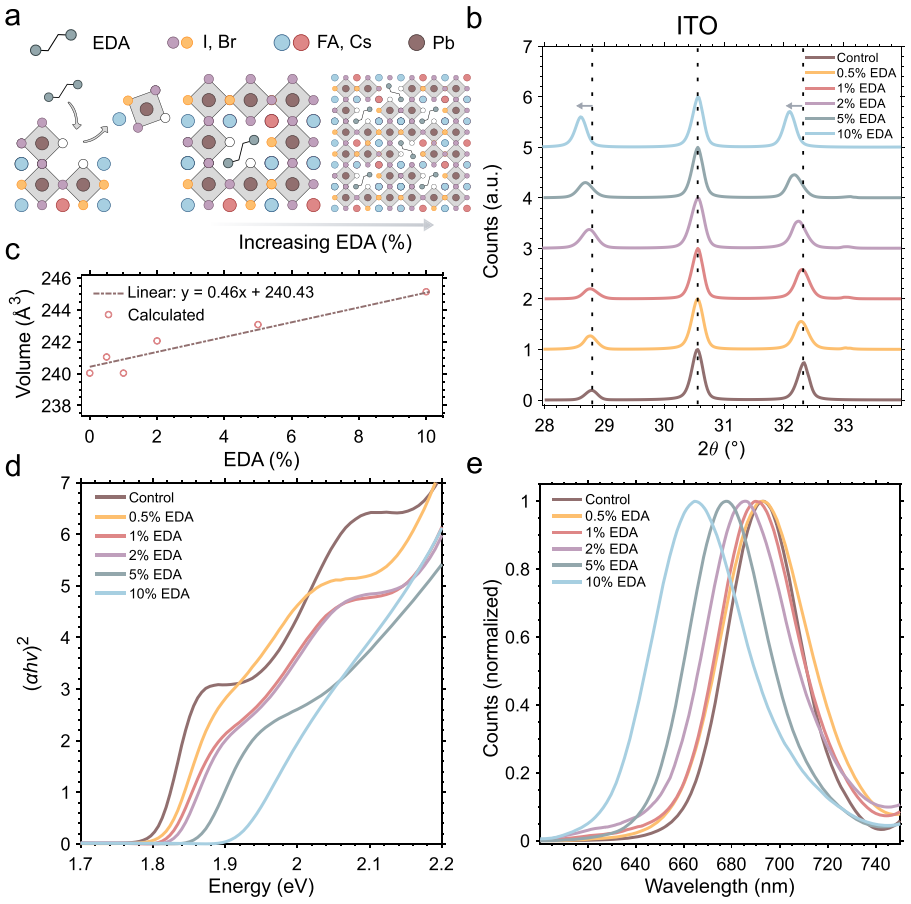

Figure 1. Hollow perovskite generation in mixed-halide thin films. a) Schematic of mixed-halide hollow perovskite structure generation. b) Thin film XRD of $Cs_{0.17}FA_{0.83}Pb(I_{0.6}Br_{0.4})_3$ perovskite with increasing EDA content. c) Unit cell volume calculated from *d* spacing extracted from (Figure S2). d) Tauc plot and e) PL emission with varying EDA content.

We used XRD and ^{1}H NMR to assess the EDA incorporation and the formation of the hollow structure. In XRD, we observe a shift to lower 2θ (expanded lattice) that increases with EDA % (Figure 1b, Supplementary Note 1). From ^{1}H NMR we see that EDA is unchanged when combined in solution with other perovskite precursors and that no reaction with FA is observed (Figures S21−S27 and Supplementary Note 2), based on which we offer that it is incorporated as EDA during perovskite film formation, forming the hollow structure. This is accompanied by a widening of the optical band gap seen as a blue shift in both UV−vis absorption and PL emission (Figure 1d,e and Figure S1) with increasing hollowness. To ascertain whether the change in band gap is due to the hollow structure rather than a change in the halide ratio, we used XPS to measure the halide ratio, finding that it varies by no more than 5% over the full range of EDA studied herein (Table S1). As seen in prior studies,[12,16] films with increasing EDA show an increase in the X:B site ratio, increasing from 4.56 for nonhollow films to 4.79 for films with 10% EDA (Table S1), indicative of the Pb^{2+} vacancies characteristic of hollow perovskites.

In order to relate the amount of hollowing agent in the precursor solution to the degree of hollowness in the final thin film, we calculated the unit cell volume by first assuming a cubic structure[18] and then calculating the cubic unit cell lattice parameter from the corresponding *d* spacings of the (001) peak in the thin film XRD (Figure S2). The calculated cubic unit cell volume exhibits a linear relationship with EDA % (Figure 1c), as also seen in previous reports.[12] We therefore use the previously established single-crystal hollow perovskite composition formula, $(A)_{1-x}(en)_x(B)_{1-0.7x}(X)_{3-0.4x}$,[12] to define the degree of hollowness in the thin film mixed-halide crystal structure: for example, adding 1% EDA to the precursor solution results in a corresponding hollow composition of $(Cs_{0.17}FA_{0.83})_{0.99}(EDA)_{0.01}(Pb)_{0.993}(I_{0.6}Br_{0.4})_{2.996}$.

To assess the ability of the hollow perovskite structure to improve photostability, we tracked the PL from films over time as a function of EDA % as a function of light intensity. The progressive red shift and broadening of PL emission, often accompanied by the appearance and growth of a low-energy shoulder (I-rich phase), are associated with demixing of the previously homogeneous mixed-halide phase.[2,7,19]

PL peak tracking was performed at 1, 3.4, and 6.9 sun equivalent illumination intensities (details in Methods) over a period of 20 min. Representative PL scans at 3.4 sun illumination intensity, along with residual PL peak analysis, are shown in Figure 2a−f, respectively, while the remainder of the scans referenced in the phase stability discussion can be found in the Supporting Information.

Films with up to 10% EDA inclusion were evaluated, since the inclusion of higher levels of EDA led to significantly decreased PL intensity (Figures S4 and S5). Without EDA, a red shift is present even after 1 min of exposure to 3.4 sun incident intensity (Figure 2a,d). The red shift and emergence of a low-energy shoulder decrease with increasing EDA concentration (Figure

https://doi.org/10.1021/acs.jpclett.3c01156
J. Phys. Chem. Lett. 2023, 14, 6157−6162

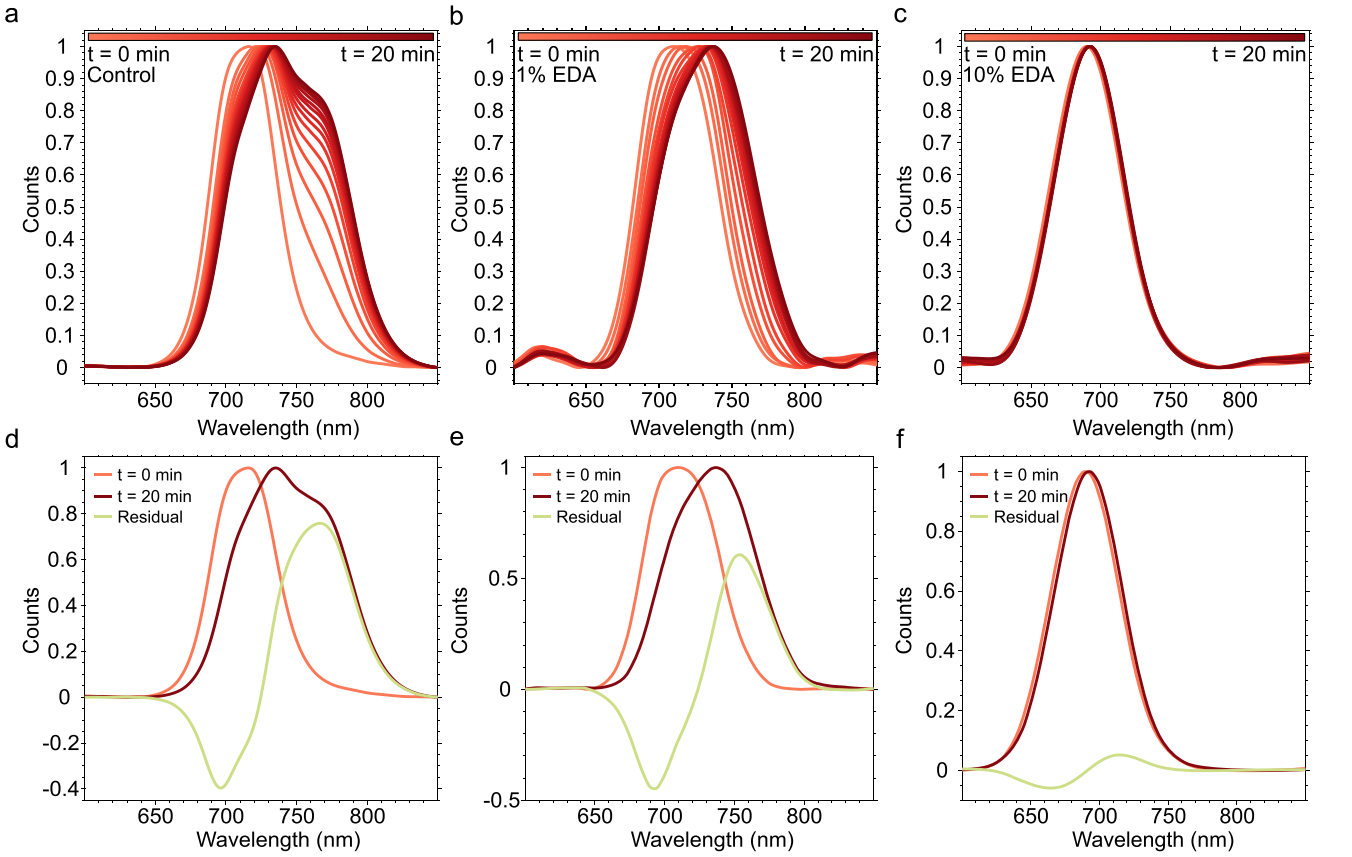

Figure 2. A hollow structure improves the photostability of $Cs_{0.17}FA_{0.83}Pb(I_{0.6}Br_{0.4})_3$ mixed-halide perovskites. a) PL peak tracking of the control composition with 3.4 sun equivalent illumination intensity over a period of 20 min. b) PL peak tracking of $(Cs_{0.17}FA_{0.83})_{0.99}(EDA)_{0.01}(Pb)_{0.993}(I_{0.6}Br_{0.4})_{2.996}$ over a period of 20 min. c) PL peak tracking of $(Cs_{0.17}FA_{0.83})_{0.9}(EDA)_{0.10}(Pb)_{0.93}(I_{0.6}Br_{0.4})_{2.96}$ over a period of 20 min. d–f) Residual PL peak analysis of a–c), respectively.

2b,c). However, at 6.9 suns, 10% EDA films do begin to red shift (Figure S7). Under 1 sun, 1% EDA is sufficient to mitigate halide segregation over the course of 20 min (Figure S8).

The photoluminescence quantum yield (PLQY) (Figure 3a) decreases by roughly 1 order of magnitude in the 1% EDA case, and this is accompanied by the expected reduction in excited-state lifetime seen in transient photoluminescence (TPL) (Figure 3c). The open circuit voltage (V_{OC}) of hollow mixed-halide perovskite solar cells (PSCs) vs increasing EDA % follows the trend expected from PL (Figures S9 and S10).

Kanatzidis and co-workers have shown that the 3D frameworks of hollow perovskites are disrupted by the presence of metal and iodide vacancies.[12] However, vacancies in lead-based perovskites are known to produce more benign in-band or shallow traps.[20,21] We offer the possibility that the changes in PLQY and TPL with hollowing may relate to trap densities at grain boundaries rather than the hollow sites themselves.

To evaluate charge transport characteristics with respect to EDA %, we used terahertz spectroscopy to probe the photoinduced conductivity and the intragrain carrier mobility.[22] The estimated charge carrier mobilities decrease linearly with increasing EDA %, from ~26 $cm^2\ V^{-1}\ s^{-1}$ in the control film to ~6 $cm^2\ V^{-1}\ s^{-1}$ in films with 10% EDA (Figure 3b). A similar linear decrease in mobility was observed for films containing 20% Br (Figure S13). The hollow structure appears to impede carrier movement within grains, likely due to the increased presence of vacancies. This is consistent with the trend in short circuit current (J_{SC}) (Figure S14).

Previous simulations have shown that ion transport in hollow perovskites exhibits a strong dependence on the degree of hollowness. In hollow $MAPbI_3$, the activation energy of migrating I vacancies increases with increasing EDA %.[15] Other studies investigating ion migration in hollow FA-based perovskites have shown that the activation energy decreases with increasing EDA %.[23] The present results for 40% Br thin films agree with the former. Since perovskites can act as an ionic conductor,[24] changes in capacitance in the low-frequency ($<10^3$ Hz) regime are associated with ion accumulation at the interface.[25,26] The decrease in capacitance in the low-frequency regime in EDA-containing mixed-halide thin films (Figure 3d) agrees with the picture of restricted ion migration, leading to increased photostability.

In summary, mixed-halide wide band gap perovskites, such as those commonly used in all-perovskite tandems (40% Br), can be stabilized by generating a hollow perovskite structure. With the increasing hollowness of the perovskite, there is further enhanced photostability, as evidenced by PL peak tracking. Terahertz spectroscopy and capacitance–frequency measurements suggest that the enhanced photostability is correlated to an increased presence of vacancies and reduced vacancy mobility induced by the hollow structure. This, we propose, may be linked to an increase in the kinetic energy required for ion migration which is consistent with a prior ion-migration

https://doi.org/10.1021/acs.jpclett.3c01156
J. Phys. Chem. Lett. 2023, 14, 6157–6162

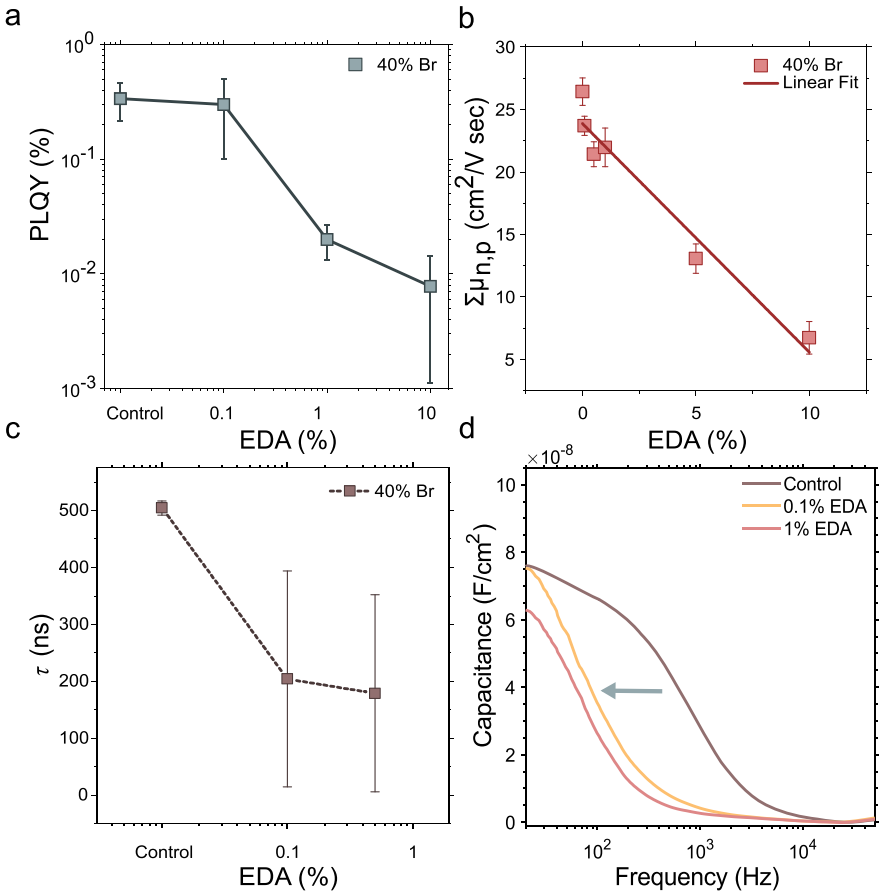

Figure 3. Impact of hollowness on the optoelectronic properties of $Cs_{0.17}FA_{0.83}Pb(I_{0.6}Br_{0.4})_3$ mixed-halide perovskites. a) Photoluminescence quantum yield (PLQY) as a function of EDA content. b) Combined carrier mobility of hollow perovskites as a function of EDA content as determined using time-resolved terahertz spectroscopy (TRTS). c) Carrier lifetimes extracted from transient photoluminescence measurements (Figure S10). d) Capacitance–frequency measurements as a function of the EDA content.

study on the iodide system.[15] Future studies on the passivation of intergrain boundary trap states may contribute to improving the device performance in these materials.

■ ASSOCIATED CONTENT

Supporting Information

The Supporting Information is available free of charge at https://pubs.acs.org/doi/10.1021/acs.jpclett.3c01156.

Materials and Methods, Supplementary Notes 1 and 2, Tables S1–S5, and Figures S1–S27 (PDF)

Transparent Peer Review report available (PDF)

■ AUTHOR INFORMATION

Corresponding Author

Edward H. Sargent − *Department of Electrical and Computer Engineering, University of Toronto, Toronto, Ontario M5S 1A4, Canada; Department of Chemistry and Department of Electrical and Computer Engineering, Northwestern University, Evanston, Illinois 60208, United States;* orcid.org/0000-0003-0396-6495; Email: ted.sargent@utoronto.ca

Authors

Luke Grater − *Department of Electrical and Computer Engineering, University of Toronto, Toronto, Ontario M5S 1A4, Canada;* orcid.org/0000-0001-5920-4022

Mingcong Wang − *King Abdullah University of Science and Technology (KAUST), KAUST Solar Center (KSC), Physical Sciences and Engineering Division (PSE), Thuwal 23955-6900, Kingdom of Saudi Arabia*

Sam Teale − *Department of Electrical and Computer Engineering, University of Toronto, Toronto, Ontario M5S 1A4, Canada;* orcid.org/0000-0001-9638-3453

Suhas Mahesh − *Department of Electrical and Computer Engineering, University of Toronto, Toronto, Ontario M5S 1A4, Canada;* orcid.org/0000-0002-3897-7963

Aidan Maxwell − *Department of Electrical and Computer Engineering, University of Toronto, Toronto, Ontario M5S 1A4, Canada*

Yanjiang Liu − *Department of Electrical and Computer Engineering, University of Toronto, Toronto, Ontario M5S 1A4, Canada;* orcid.org/0000-0002-6119-2793

So Min Park − *Department of Electrical and Computer Engineering, University of Toronto, Toronto, Ontario M5S 1A4, Canada*

Bin Chen − *Department of Electrical and Computer Engineering, University of Toronto, Toronto, Ontario M5S 1A4, Canada; Department of Chemistry, Northwestern University, Evanston, Illinois 60208, United States;* orcid.org/0000-0002-2106-7664

Frédéric Laquai − *King Abdullah University of Science and Technology (KAUST), KAUST Solar Center (KSC), Physical Sciences and Engineering Division (PSE), Thuwal 23955-*

https://doi.org/10.1021/acs.jpclett.3c01156
J. Phys. Chem. Lett. 2023, 14, 6157−6162

6900, Kingdom of Saudi Arabia; orcid.org/0000-0002-5887-6158

Mercouri G. Kanatzidis − *Department of Chemistry, Northwestern University, Evanston, Illinois 60208, United States;* orcid.org/0000-0003-2037-4168

Complete contact information is available at: https://pubs.acs.org/10.1021/acs.jpclett.3c01156

Author Contributions

Conceptualization: L.G. Methodology: L.G., S.T., S.M., A.M., S.M.P., and B.C. Thin film fabrication: L.G. Device fabrication: L.G. X-ray diffraction: L.G. Spectroscopy: L.G., M.W., and Y.L. Supervision: E.H.S., M.G.K., and F.L.

Notes

The authors declare no competing financial interest.

■ ACKNOWLEDGMENTS

This research was made possible by the U.S. Department of the Navy, Office of Naval Research (grant N00014-20-1-2572). M.G.K. was supported in part by grant SC0012541 from the U.S. Department of Energy, Office of Science. This publication is based upon work supported by the King Abdullah University of Science and Technology (KAUST) Office of Sponsored Research (OSR) under Award No: OSR-CARF/CCF-3079, OSR-2019-CRG8-4093, and OSR-2020-CRG9-4350. L.G. thanks the University of Toronto CSICOMP NMR Facility for their assistance with ^{1}H NMR characterization.

■ REFERENCES

(1) Bischak, C. G.; Hetherington, C. L.; Wu, H.; Aloni, S.; Ogletree, D. F.; Limmer, D. T.; Ginsberg, N. S. Origin of Reversible Photoinduced Phase Separation in Hybrid Perovskites. *Nano Lett.* **2017**, *17* (2), 1028−1033.

(2) Hoke, E. T.; Slotcavage, D. J.; Dohner, E. R.; Bowring, A. R.; Karunadasa, H. I.; McGehee, M. D. Reversible Photo-Induced Trap Formation in Mixed-Halide Hybrid Perovskites for Photovoltaics. *Chem. Sci.* **2015**, *6* (1), 613−617.

(3) Yoon, S. J.; Draguta, S.; Manser, J. S.; Sharia, O.; Schneider, W. F.; Kuno, M.; Kamat, P. V. Tracking Iodide and Bromide Ion Segregation in Mixed Halide Lead Perovskites during Photoirradiation. *ACS Energy Lett.* **2016**, *1* (1), 290−296.

(4) Brennan, M. C.; Draguta, S.; Kamat, P. V.; Kuno, M. Light-Induced Anion Phase Segregation in Mixed Halide Perovskites. *ACS Energy Lett.* **2018**, *3* (1), 204−213.

(5) Leijtens, T.; Bush, K. A.; Prasanna, R.; McGehee, M. D. Opportunities and Challenges for Tandem Solar Cells Using Metal Halide Perovskite Semiconductors. *Nature Energy* **2018**, *3* (10), 828−838.

(6) Barker, A. J.; Sadhanala, A.; Deschler, F.; Gandini, M.; Senanayak, S. P.; Pearce, P. M.; Mosconi, E.; Pearson, A. J.; Wu, Y.; Srimath Kandada, A. R.; et al. Defect-Assisted Photoinduced Halide Segregation in Mixed-Halide Perovskite Thin Films. *ACS Energy Lett.* **2017**, *2* (6), 1416−1424.

(7) Knight, A. J.; Borchert, J.; Oliver, R. D. J.; Patel, J. B.; Radaelli, P. G.; Snaith, H. J.; Johnston, M. B.; Herz, L. M. Halide Segregation in Mixed-Halide Perovskites: Influence of A-Site Cations. *ACS Energy Lett.* **2021**, *6* (2), 799−808.

(8) Xu, J.; Boyd, C. C.; Yu, Z. J.; Palmstrom, A. F.; Witter, D. J.; Larson, B. W.; France, R. M.; Werner, J.; Harvey, S. P.; Wolf, E. J.; et al. Triple-Halide Wide-Band Gap Perovskites with Suppressed Phase Segregation for Efficient Tandems. *Science* **2020**, *367* (6482), 1097−1104.

(9) Al-Ashouri, A.; Köhnen, E.; Li, B.; Magomedov, A.; Hempel, H.; Caprioglio, P.; Márquez, J. A.; Morales Vilches, A. B.; Kasparavicius, E.; Smith, J. A.; et al. Monolithic Perovskite/Silicon Tandem Solar Cell with > 29% Efficiency by Enhanced Hole Extraction. *Science* **2020**, *370* (6522), 1300−1309.

(10) Liu, J.; Aydin, E.; Yin, J.; De Bastiani, M.; Isikgor, F. H.; Rehman, A. U.; Yengel, E.; Ugur, E.; Harrison, G. T.; Wang, M.; et al. 28.2%-Efficient, Outdoor-Stable Perovskite/Silicon Tandem Solar. *Cell. Joule* **2021**, *5* (12), 3169−3186.

(11) Sherkar, T. S.; Momblona, C.; Gil-Escrig, L.; Ávila, J.; Sessolo, M.; Bolink, H. J.; Koster, L. J. A. Recombination in Perovskite Solar Cells: Significance of Grain Boundaries, Interface Traps, and Defect Ions. *ACS Energy Lett.* **2017**, *2* (5), 1214−1222.

(12) Spanopoulos, I.; Ke, W.; Stoumpos, C. C.; Schueller, E. C.; Kontsevoi, O. Y.; Seshadri, R.; Kanatzidis, M. G. Unraveling the Chemical Nature of the 3D "Hollow" Hybrid Halide Perovskites. *J. Am. Chem. Soc.* **2018**, *140* (17), 5728−5742.

(13) Spanopoulos, I.; Hadar, I.; Ke, W.; Guo, P.; Mozur, E. M.; Morgan, E.; Wang, S.; Zheng, D.; Padgaonkar, S.; Manjunatha Reddy, G. N.; et al. Tunable Broad Light Emission from 3D "Hollow" Bromide Perovskites through Defect Engineering. *J. Am. Chem. Soc.* **2021**, *143* (18), 7069−7080.

(14) Ke, W.; Stoumpos, C. C.; Zhu, M.; Mao, L.; Spanopoulos, I.; Liu, J.; Kontsevoi, O. Y.; Chen, M.; Sarma, D.; Zhang, Y.; et al. Enhanced Photovoltaic Performance and Stability with a New Type of Hollow 3D Perovskite {en}FASnI3. *Sci Adv* **2017**, *3* (8), e1701293.

(15) Senocrate, A.; Spanopoulos, I.; Zibouche, N.; Maier, J.; Islam, M. S.; Kanatzidis, M. G. Tuning Ionic and Electronic Conductivities in the "Hollow" Perovskite *en*MAPbI$_3$. *Chem. Mater.* **2021**, *33* (2), 719−726.

(16) Worku, M.; Tian, Y.; Zhou, C.; Lin, H.; Chaaban, M.; Xu, L.-J.; He, Q.; Beery, D.; Zhou, Y.; Lin, X.; et al. Hollow Metal Halide Perovskite Nanocrystals with Efficient Blue Emissions. *Sci. Adv.* **2020**, *6* (17), eaaz5961.

(17) Knight, A. J.; Wright, A. D.; Patel, J. B.; McMeekin, D. P.; Snaith, H. J.; Johnston, M. B.; Herz, L. M. Electronic Traps and Phase Segregation in Lead Mixed-Halide Perovskite. *ACS Energy Lett.* **2019**, *4* (1), 75−84.

(18) Rehman, W.; McMeekin, D. P.; Patel, J. B.; Milot, R. L.; Johnston, M. B.; Snaith, H. J.; Herz, L. M. Photovoltaic Mixed-Cation Lead Mixed-Halide Perovskites: Links between Crystallinity, Photo-Stability and Electronic Properties. *Energy Environ. Sci.* **2017**, *10* (1), 361−369.

(19) Beal, R. E.; Hagström, N. Z.; Barrier, J.; Gold-Parker, A.; Prasanna, R.; Bush, K. A.; Passarello, D.; Schelhas, L. T.; Brüning, K.; Tassone, C. J.; et al. Structural Origins of Light-Induced Phase Segregation in Organic-Inorganic Halide Perovskite Photovoltaic. *Materials. Matter* **2020**, *2* (1), 207−219.

(20) Jin, H.; Debroye, E.; Keshavarz, M.; Scheblykin, I. G.; Roeffaers, M. B. J.; Hofkens, J.; Steele, J. A. It's a Trap! On the Nature of Localised States and Charge Trapping in Lead Halide Perovskites. *Mater. Horiz.* **2020**, *7* (2), 397−410.

(21) Buin, A.; Pietsch, P.; Xu, J.; Voznyy, O.; Ip, A. H.; Comin, R.; Sargent, E. H. Materials Processing Routes to Trap-Free Halide Perovskites. *Nano Lett.* **2014**, *14* (11), 6281−6286.

(22) Lin, R.; Xu, J.; Wei, M.; Wang, Y.; Qin, Z.; Liu, Z.; Wu, J.; Xiao, K.; Chen, B.; Park, S. M.; et al. All-Perovskite Tandem Solar Cells with Improved Grain Surface Passivation. *Nature* **2022**, *603* (7899), 73−78.

(23) Jayanthi, K.; Spanopoulos, I.; Zibouche, N.; Voskanyan, A. A.; Vasileiadou, E. S.; Islam, M. S.; Navrotsky, A.; Kanatzidis, M. G. Entropy Stabilization Effects and Ion Migration in 3D "Hollow" Halide Perovskites. *J. Am. Chem. Soc.* **2022**, *144* (18), 8223−8230.

(24) Awni, R. A.; Song, Z.; Chen, C.; Li, C.; Wang, C.; Razooqi, M. A.; Chen, L.; Wang, X.; Ellingson, R. J.; Li, J. V.; et al. Influence of Charge Transport Layers on Capacitance Measured in Halide Perovskite Solar Cells. *Joule* **2020**, *4* (3), 644−657.

(25) Almora, O.; Zarazua, I.; Mas-Marza, E.; Mora-Sero, I.; Bisquert, J.; Garcia-Belmonte, G. Capacitive Dark Currents, Hysteresis, and Electrode Polarization in Lead Halide Perovskite Solar Cells. *J. Phys. Chem. Lett.* **2015**, *6* (9), 1645−1652.

(26) Futscher, M. H.; Gangishetty, M. K.; Congreve, D. N.; Ehrler, B. Quantifying Mobile Ions and Electronic Defects in Perovskite-Based

Devices with Temperature-Dependent Capacitance Measurements: Frequency vs Time Domain. *J. Chem. Phys.* **2020**, *152* (4), 044202.

https://doi.org/10.1021/acs.jpclett.3c01156
J. Phys. Chem. Lett. 2023, 14, 6157−6162